ELSEVIER

Journal of Power Sources 79 (1999) 19–24

JOURNAL OF POWER SOURCES

Effect of temperature on the discharge capacity of the Laves phase alloy used in nickel/metal-hydride batteries

Chigyu Jeong [a,*], Wonsub Chung [a], Chiaki Iwakura [b], Ingon Kim [c]

[a] *Department of Metallurgical Engineering, Pusan National University, Pusan, 609-735, South Korea*
[b] *Department of Applied Chemistry, College of Engineering, Osaka Prefecture University, Sakai, Osaka, 599-8531, Japan*
[c] *Department of Materials Engineering, Dongeui University, Pusan, 614-714, South Korea*

Received 20 August 1998; accepted 22 October 1998

Abstract

The discharge capacity, the high-rate dischargeability and the self-discharge characteristics of negative electrodes consisting of the Zr-based, modified AB_2 type alloys of $ZrV_{0.1}Mn_{0.7}Ni_{1.2}$ alloy and $ZrV_{0.1}Mn_{0.5}Mo_{0.2}Ni_{1.2}$ alloy, the latter having the form of partially substituted Mo for Mn sites in the former alloy, are investigated in 6 M KOH solution at 30, 40 and 60°C. It is found that the discharge capacities obtained at 30 and 40°C are almost the same in both alloys, but they decrease at 60°C. The activation process becomes faster in both alloys with increasing temperature. The high-rate dischargeability increases slightly from 85% at 30°C to 90% at 60°C. At the very high discharge current of 5 A g^{-1}, however, the discharge capacity at 60°C was increased by 7 × and 17 × more than that at 30°C in $ZrV_{0.1}Mn_{0.7}Ni_{1.2}$ alloy and $ZrV_{0.1}Mn_{0.5}Mo_{0.2}Ni_{1.2}$ alloy, respectively. The addition of Mo improved the self-discharge characteristics, especially at 60°C.

Keywords: Nickel/metal-hydride battery; Laves phase alloy; Activation; Capacity; High-rate dischargeability; Self-discharge

1. Introduction

Recently, extensive studies on ZrV_2 Laves phase alloys have been conducted for the purpose of adopting them as negative electrode materials in nickel/metal-hydride (Ni–MH) batteries because of their discharge capacities (theoretical discharge capacity of $ZrV_2 = 763$ mA h g^{-1}) are higher than those of rare-earth type hydrogen-storage alloys ($LaNi_5 = 372$ mA h g^{-1}). Despite such a high discharge capacity, the activation process, high-rate capability and self-discharge characteristics, especially at high temperature, are rather poor. One strategy for the improvement of these properties is to substitute other elements such as Ni and Mn for the V site to lower the heat of hydride formation ($-\Delta H_f°$). It has been reported that a discharge capacity over 400 mA h g^{-1} can be obtained in V–Ti–Mn–Ni and Zr–V–Mn–Ni alloys [1–3]. On the other hand, the high-rate dischargeability and the self-discharge rate of Ni–MH batteries using AB_2 Laves alloys are poor compared with those of the Ni–Cd battery. This is mainly due to the negative electrode material's characteristics, which have to be improved to provide practical electrode material [4].

In this study, the activation process, high-rate capability and self-discharge characteristics from 30 to 60°C are investigated with a $ZrV_{0.1}Mn_{0.7}Ni_{1.2}$ Laves phase alloy. The effect of partial substitution of Mo for Mn sites ($ZrV_{0.1}Mn_{0.5}Mo_{0.2}Ni_{1.2}$) on these properties is also examined.

2. Experimental

$ZrV_{0.1}Mn_{0.7}Ni_{1.2}$ Laves phase alloy and $ZrV_{0.1}Mn_{0.5}Mo_{0.2}Ni_{1.2}$ alloy were prepared by arc melting under an argon atmosphere. After mechanical pulverization of the alloys, about 100 mg of the alloy powder (size: 106 to 125 μm) was mixed with polyvinyl alcohol solution as binder. The negative electrode was prepared by filling a porous nickel substrate with the mixture, vacuum drying at 120°C for 1 h and then pressing at 600 kgf cm^{-2}.

Charge–discharge cycle tests were conducted using a three-compartment cell made of pyrex-glass in which the negative electrode was set in the central compartment and

* Corresponding author

0378-7753/99/$ - see front matter
PII: S0378-7753(98)00176-1

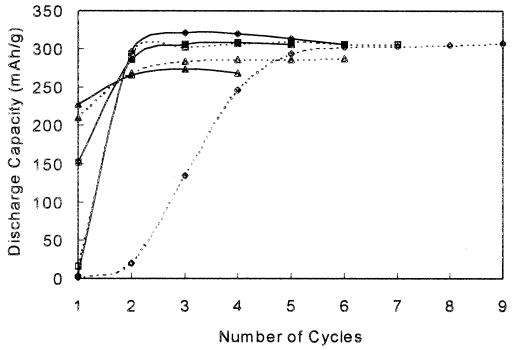

Fig. 1. Activation profiles of $ZrV_{0.1}Mn_{0.7}Ni_{1.2}$ and $ZrV_{0.1}Mn_{0.5}Mo_{0.2}Ni_{1.2}$ electrodes at various temperatures. $ZrV_{0.1}Mn_{0.7}Ni_{1.2}$: ◆ 30°C, ■ 40°C, ▲ 60°C; $ZrV_{0.1}Mn_{0.5}Mo_{0.2}Ni_{1.2}$: ◇ 30°C, □ 40°C, △ 60°C.

a platinum positive electrode was placed either side. The electrolyte was 6 M KOH and was de-aerated by argon gas bubbling. A mercury oxide electrode (Hg/HgO/6 M KOH) was used as a reference electrode. Galvanostatic charging (20 mA) and discharging (5 mA) modes (HOKUDO DENKO HJ201B) were repeated until the discharge capacity of the negative electrode reached its saturation value. There was a rest period of 10 min after charge. The discharge was continued until the potential reached −0.5 V vs. Hg/HgO/6 M KOH reference electrode. The cell temperature was maintained at 30, 40 and 60°C by means of a water bath.

In this work, the high-rate dischargeability (HRD) was defined by the following equation:

$$\text{high-rate dischargeability}\,(\%) = C_{50}/[C_{50} + C_5 + C_2] \times 100 \quad (1)$$

where C_{50} is the discharge capacity at a discharge current of 50 mA (~ 500 mA g^{-1}), C_5 is the additional discharge capacity at a discharge current of 5 mA measured after 10 min of the rest period following the measurement of C_{50}, and C_2 is the additional discharge capacity at a discharge current of 2 mA following the measurement of C_5.

The rate capability of the electrode was also investigated by measuring the discharge capacities at discharge currents of 25 mA g^{-1}, 250 mA g^{-1}, 1 A g^{-1}, 2.5 A g^{-1} and 5 A g^{-1} and at 30, 40 and 60°C.

The exchange-current density (J_o) was determined from the slope (η/J) of the polarization curve taken in the vicinity of the rest potential by the linear polarization method (EG&G Potentiostat/Galvanostat Model 273) after charging at 20 mA for 5 min using the following equation:

$$\eta/J = [RT]/[J_o F] \quad (2)$$

The self-discharge characteristics of the negative electrodes were determined by charge retention (%), which is expressed as the ratio of the discharge capacity after 7 days under open-circuit conditions at 30, 40 and 60°C to the saturated discharge capacity.

Electrochemical pressure-composition isotherms [5] at 30, 40 and 60°C were determined by measurement of the rest electrode potential after discharging a fully charged electrode by a small amount of electric charge. This procedure was repeated until the electrode was completely discharged. According to the Nernst equation, the potential of the negative electrode at an equilibrium state, E (V), corresponds to the hydrogen gas pressure on the surface which is equilibrated with atomic hydrogen in the hydride ($H_2 = 2H$) as follows:

$$E = E^o - [RT]/[nF]\ln\left[a_{H_2O}/\left(\gamma_{H_2}P_{H_2}\right)\right] \quad (3)$$

where: E^o is the standard electrode potential (V); a_{H_2O} is the activity of water; γ_{H_2} is the fugacity coefficient; P_{H_2} is the hydrogen partial pressure (bar). The hydrogen pressure was calculated from the equilibrium potentials using the electrochemical data in a concentrated KOH solution reported by Balej [6].

From the pressure-composition isotherms, the enthalpy change for hydride formation ($-\Delta H_f^\circ$) was calculated by following equation derived from the van't Hoff equation:

$$\ln p_{H_2} = 2\Delta H_f^\circ/[xRT] - 2\Delta S_f^\circ/[xR] \quad (4)$$

where: p_{H_2} is the plateau pressure (atm) at a given temperature; x is the number of hydrogen atoms per formula unit of hydrogen-storage alloy.

The crystal structure of the two alloys was studied by means of X-ray diffractometry using Cu K_α radiation. Cross-sectional views of the electrodes after activation were observed using a scanning electron microscope (SEM). The hardness of the alloy was measured with a Microvickers hardness tester.

3. Results and discussion

3.1. Activation profiles

The discharge capacities of the two types of electrode with charge–discharge cycling are shown in Fig. 1. For

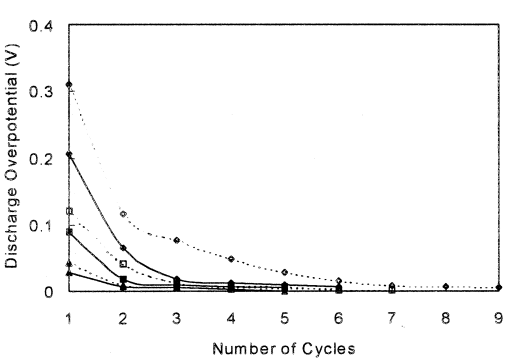

Fig. 2. Changes in discharge overpotentials of $ZrV_{0.1}Mn_{0.7}Ni_{1.2}$ and $ZrV_{0.1}Mn_{0.5}Mo_{0.2}Ni_{1.2}$ electrodes at various temperatures. $ZrV_{0.1}Mn_{0.7}Ni_{1.2}$: ◆ 30°C, ■ 40°C, ▲ 60°C; $ZrV_{0.1}Mn_{0.5}Mo_{0.2}Ni_{1.2}$: ◇ 30°C, □ 40°C, △ 60°C.

both electrodes, the number of cycles required to reach the saturated discharge capacity value decreases with increasing temperature. It is noticeable that the discharge capacity of the two types of electrodes reaches ~230 mA h g^{-1} at 60°C, even in the first cycle. The $ZrV_{0.1}Mn_{0.7}Ni_{1.2}$ alloy is more easily activated than the alloy containing Mo at 30°C, whereas its discharge capacity decreases from 320 mA h g^{-1} at 30°C to 270 mA h g^{-1} at 60°C. After reaching the maximum discharge capacity, the electrode starts to lose some of its discharge capacity. In case of the $ZrV_{0.1}Mn_{0.5}Mo_{0.2}Ni_{1.2}$ alloy, the activation at 60°C becomes comparable with the former alloy. Also this alloy exhibited better maintenance of saturated discharge capacity than the other alloy at 60°C.

In order to reach the maximum discharge capacity, a fresh electrode generally needs a few charge–discharge

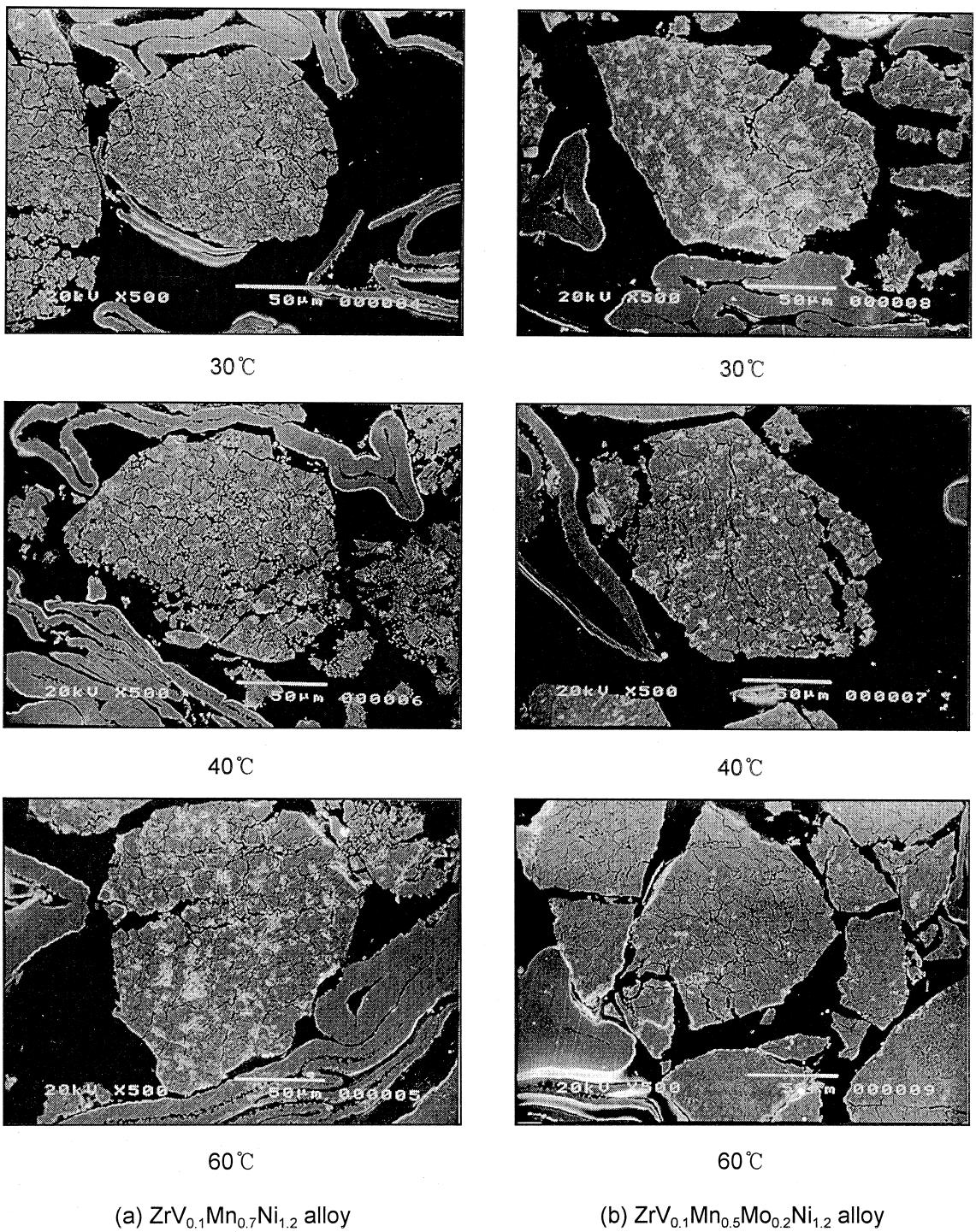

Fig. 3. Cross-sectional view of (a) $ZrV_{0.1}Mn_{0.7}Ni_{1.2}$ alloy and (b) $ZrV_{0.1}Mn_{0.5}Mo_{0.2}Ni_{1.2}$ alloy after activation by SEM at 30, 40 and 60°C.

cycles to eliminate any existing oxide layer or absorbed gas on the alloy surface that interferes with the penetration of hydrogen into the lattice [7]. Also, the appearance of an oxide-free surface resulting from pulverization of the alloy particles during cycling facilitates the activation process. This process was further investigated by measuring the overpotential during cycling, see Fig. 2. The cycle number at zero overpotential corresponds to that needed for electrode activation. Since the overpotential is related to the reduction of any oxide film on the alloy surface, this fact indicates that any obstacles which prevent the penetration of the hydrogen are completely removed when the electrode is fully activated. It is also seen that the overpotential decreases with increasing temperature. The difference in overpotential of the two alloys appears to be related to their oxide characteristics.

Since the surface area of the particles also plays a significant role in the activation stage, cross-sectional views of the electrode particles were photographed (Fig. 3) to elucidate the difference in the activation behaviour of the two alloys. More cracks are seen in $ZrV_{0.1}Mn_{0.7}Ni_{1.2}$ alloy. The Microvickers hardness of this alloy and its counterpart is 730 and 667, respectively. Therefore, crack formation seems to be more favorable in the alloy possessing the higher hardness. Thus, the larger oxide-free surface area formed on $ZrV_{0.1}Mn_{0.7}Ni_{1.2}$ alloy results in a low overpotential and shortens the activation cycles.

3.2. High-rate dischargeability (HRD)

The HRD of the two alloys is nearly the same at all temperatures and increases with increasing temperature from 85% at 30°C to 90% at 60°C. This increase can be explained by the increase in the apparent exchange-current density with increasing temperature, as shown in Fig. 4. It is seen that the HRD increases linearly with the apparent exchange-current density. As the exchange-current density is related to the electrocatalytic activity of the negative electrode, this result indicates that the discharge reaction is controlled by the surface reaction [8].

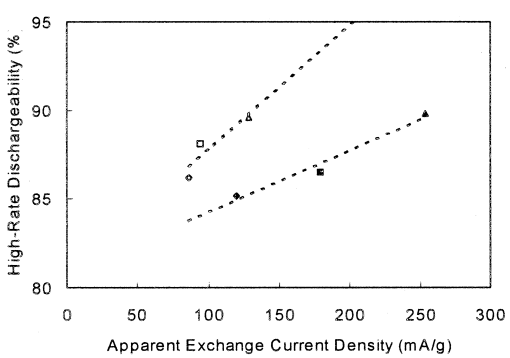

Fig. 4. High-rate dischargeability vs. apparent exchange-current density of $ZrV_{0.1}Mn_{0.7}Ni_{1.2}$ and $ZrV_{0.1}Mn_{0.5}Mo_{0.2}Ni_{1.2}$ electrodes at various temperatures. $ZrV_{0.1}Mn_{0.7}Ni_{1.2}$: ♦ 30°C, ■ 40°C, ▲ 60°C; $ZrV_{0.1}Mn_{0.5}Mo_{0.2}Ni_{1.2}$: ◇ 30°C, □ 40°C, △ 60°C.

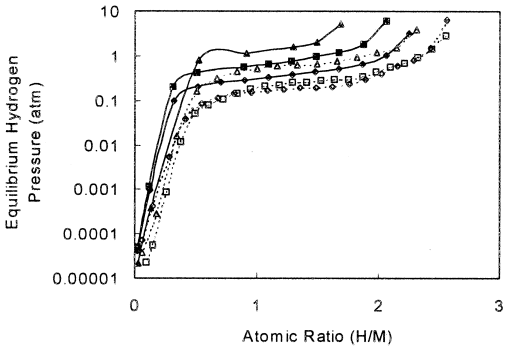

Fig. 5. Electrochemical pressure-composition isotherms of $ZrV_{0.1}Mn_{0.7}Ni_{1.2}$ and $ZrV_{0.1}Mn_{0.5}Mo_{0.2}Ni_{1.2}$ electrodes at various temperatures. $ZrV_{0.1}Mn_{0.7}Ni_{1.2}$: ♦ 30°C, ■ 40°C, ▲ 60°C; $ZrV_{0.1}Mn_{0.5}Mo_{0.2}Ni_{1.2}$: ◇ 30°C, □ 40°C, △ 60°C.

The higher value of the apparent exchange-current density for the $ZrV_{0.1}Mn_{0.7}Ni_{1.2}$ alloy compared with that of the $ZrV_{0.1}Mn_{0.5}Mo_{0.2}Ni_{1.2}$ alloy is due to the larger surface area. As was mentioned before, this alloy was pulverized more than the alloy containing Mo.

It has been reported [9] that the HRD increases with decreasing values of the heat of hydride formation $(-\Delta H_f^\circ)$ and of the unit cell volume in $ZrV_{2-x-y}Mn_xNi_y$ $(x = 0.2–0.8,\ y = 1.0,\ 1.2,\ 1.4)$. In this experiment, the electrochemically measured $-\Delta H_f^\circ$ and the unit cell volume (FCC structure) measured by the X-ray diffraction pattern are 38.4 kJ/mol H_2 and 350.9 Å^3 in the $ZrV_{0.1}Mn_{0.7}Ni_{1.2}$ alloy, respectively. The corresponding values are 33.8 kJ/mol H_2 and 357.7 Å^3 in the $ZrV_{0.1}Mn_{0.5}Mo_{0.2}Ni_{1.2}$ alloy. The electrochemical pressure-composition isotherms and X-ray diffraction data are shown in Figs. 5 and 6, respectively. The addition of the Mo in Mn sites results in a decrease in the heat of hydride formation and an increase in the unit cell volume. The increase in the unit cell volume can be easily understood from the size of the two atoms, i.e., Mn (1.26 Å), Mo (1.39 Å). Thus, the two counteracting effects of the addition of Mo do not affect the HRD value.

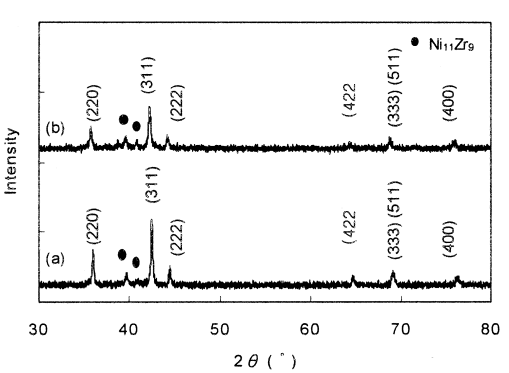

Fig. 6. X-ray diffraction patterns of (a) $ZrV_{0.1}Mn_{0.7}Ni_{1.2}$ alloy and (b) $ZrV_{0.1}Mn_{0.5}Mo_{0.2}Ni_{1.2}$ alloy.

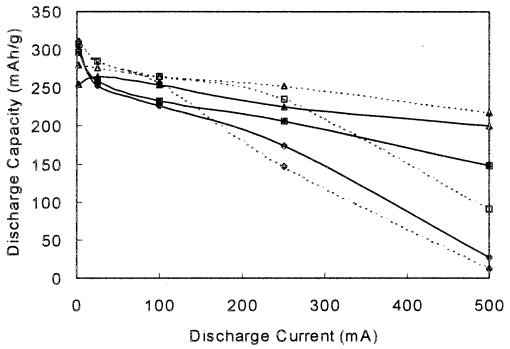

Fig. 7. Dependence of capacity on discharge current for $ZrV_{0.1}Mn_{0.7}Ni_{1.2}$ and $ZrV_{0.1}Mn_{0.5}Mo_{0.2}Ni_{1.2}$ electrodes at various temperatures. $ZrV_{0.1}Mn_{0.7}Ni_{1.2}$: ♦ 30°C, ■ 40°C, ▲ 60°C; $ZrV_{0.1}Mn_{0.5}Mo_{0.2}Ni_{1.2}$: ◇ 30°C, □ 40°C, △ 60°C.

3.3. Rate capability

In order to examine the rate capability over a wide range of current values, the discharge current was varied from 2.5 to 500 mA. The discharge capacity as a function of discharge current is shown in Fig. 7. A significant difference in discharge capacity with temperature is seen as the discharge current increases. This difference was not observed in the HRD result, in which the discharge current was 50 mA. At each discharge current, the discharge capacity increases with temperature. At 500 mA, the discharge capacity of the $ZrV_{0.1}Mn_{0.7}Ni_{1.2}$ alloy at 30°C is only about 28 mA h g^{-1}, whereas it increases to 200 mA h g^{-1} at 60°C. In $ZrV_{0.1}Mn_{0.5}Mo_{0.2}Ni_{1.2}$ alloy, it increases from 13 to 218 mA h g^{-1}. Therefore, these alloys exhibit good rate capability at high temperature. Such an increase in discharge capacity seems to be related to the diffusivity of the hydrogen and the electrocatalytic activity, both of which increase with increasing temperature.

The data were replotted in the form of log (discharge time) vs. log (discharge current), see Fig. 8 (Peukert plot). It is seen that the deviation from linearity starts only at 500 mA for the $ZrV_{0.1}Mn_{0.7}Ni_{1.2}$ alloy at 30°C. In the case of the $ZrV_{0.1}Mn_{0.5}Mo_{0.2}Ni_{1.2}$ alloy, the deviation is observed at 30°C as well as at 40°C at 250 and 500 mA, respectively. Since the linearity of the Peukert plot [10] is indicative of the capability of the negative electrode to be efficiently discharged, the $ZrV_{0.1}Mn_{0.7}Ni_{1.2}$ alloy has a better rate capability at low temperature.

Table 1
Slope of the Peukert plots

	30°C	40°C	60°C
$ZrV_{0.1}Mn_{0.7}Ni_{1.2}$	−1.32	−1.12	−1.04
$ZrV_{0.1}Mn_{0.5}Mo_{0.2}Ni_{1.2}$	−1.42	−1.16	−1.04

The slope of the curve is shown in Table 1. As the temperature increases, the slope of the Peukert plot increases. The slope for the $ZrV_{0.1}Mn_{0.7}Ni_{1.2}$ alloy is slightly higher than that for the $ZrV_{0.1}Mn_{0.5}Mo_{0.2}Ni_{1.2}$ alloy, except at 60°C. It is easily understood that the steeper the slope, the poorer the rate capability becomes.

According to these results, it can be concluded that the rate capability of $ZrV_{0.1}Mn_{0.7}Ni_{1.2}$ alloy is better than that of $ZrV_{0.1}Mn_{0.5}Mo_{0.2}Ni_{1.2}$ alloy at both 30 and 40°C.

3.4. Self-discharge

The charge retention (%), which represents the self-discharge characteristics of the electrodes stored at various temperatures, is shown in Fig. 9, together with the plateau pressure measured by the electrochemical pressure-composition isotherms. The charge retention decreases with increasing temperature, which means that hydrogen in the lattice escapes easily at higher temperature. The $ZrV_{0.1}Mn_{0.5}Mo_{0.2}Ni_{1.2}$ alloy is seen to suffer less self-discharge than the $ZrV_{0.1}Mn_{0.7}Ni_{1.2}$ alloy over the whole temperature range. The self-discharge rate of the $ZrV_{0.1}Mn_{0.7}Ni_{1.2}$ alloy becomes very high at 60°C.

As shown in Fig. 5, the plateau pressure increases with increasing temperature. The $ZrV_{0.1}Mn_{0.5}Mo_{0.2}Ni_{1.2}$ alloy

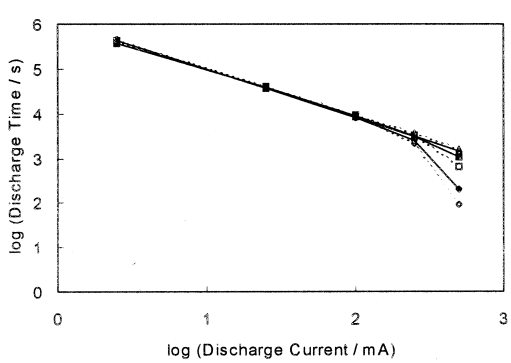

Fig. 8. Peukert plots of $ZrV_{0.1}Mn_{0.7}Ni_{1.2}$ and $ZrV_{0.1}Mn_{0.5}Mo_{0.2}Ni_{1.2}$ electrodes at various temperatures. $ZrV_{0.1}Mn_{0.7}Ni_{1.2}$: ♦ 30°C, ■ 40°C, ▲ 60°C; $ZrV_{0.1}Mn_{0.5}Mo_{0.2}Ni_{1.2}$: ◇ 30°C, □ 40°C, △ 60°C.

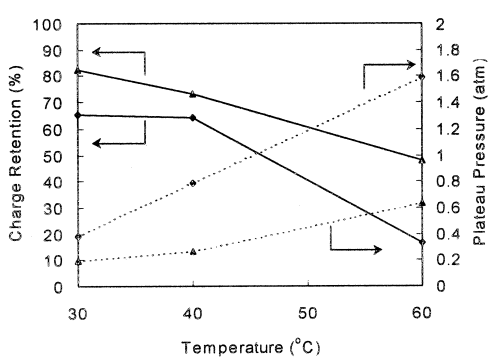

Fig. 9. Temperature dependence of charge retention and plateau pressure of $ZrV_{0.1}Mn_{0.7}Ni_{1.2}$ (♦) and $ZrV_{0.1}Mn_{0.5}Mo_{0.2}Ni_{1.2}$ (▲) electrodes.

has a lower plateau pressure than the $ZrV_{0.1}Mn_{0.7}Ni_{1.2}$ alloy over the whole temperature range. It is noticeable that the plateau pressure of the $ZrV_{0.1}Mn_{0.7}Ni_{1.2}$ alloy becomes greater than 1 atm at 60°C.

It is known that self-discharge occurs through the following two reasons [11]. First, it occurs when the equilibrium hydrogen pressure is higher than the cell inner pressure. The amount of hydrogen charged above the cell inner pressure will be easily released from the metal- hydrides resulting in loss of discharge capacity. Furthermore, NiOOH positive electrodes make the cell inner pressure lower because of the chemical reaction of hydrogen with NiOOH electrodes that results in the formation of $Ni(OH)_2$. This drop in cell inner pressure will also contribute to the self-discharge. The other cause of self-discharge is the deterioration of the negative electrodes due to the chemical or electrochemical oxidation of the alloy.

In our experiments, the possibility of the effect of the NiOOH positive electrode on the self-discharge can be rejected because platinum mesh was used as the positive electrodes. The decrease of charge retention with increasing temperature, as shown in Fig. 9, can now be explained by the fact that, at high temperature, the plateau pressure increases and thereby the rate of dissociation of hydride increases alongwith an enhanced hydrogen diffusion rate at high temperature.

The high self-discharge rate of the $ZrV_{0.1}Mn_{0.7}Ni_{1.2}$ alloy seems to be due to its higher plateau pressure, compared with that of the $ZrV_{0.1}Mn_{0.5}Mo_{0.2}Ni_{1.2}$ alloy. Thus, the largest drop in the charge retention at 60°C in $ZrV_{0.1}Mn_{0.7}Ni_{1.2}$ alloy is due to the highest plateau pressure of 1.59 atm.

4. Conclusions

From the above results, the effect of temperature on the $ZrV_{0.1}Mn_{0.7}Ni_{1.2}$ alloy electrode and the $ZrV_{0.1}Mn_{0.5}Mo_{0.2}Ni_{1.2}$ alloy electrode can be summarized as follows:

(i) As the temperature increases, the discharge capacity of the electrode decreases, but the electrodes are easily activated.

(ii) The HRD is the same and increases from 85% at 30°C to 90% at 60°C in both alloys.

(iii) At temperatures below 60°C, the rate capability of the $ZrV_{0.1}Mn_{0.7}Ni_{1.2}$ alloy electrode is superior to that of the $ZrV_{0.1}Mn_{0.5}Mo_{0.2}Ni_{1.2}$ alloy electrode.

(iv) The addition of Mo improves the self-discharge characteristics over the whole temperature range.

Acknowledgements

Korea Ministry of Education in 1997 supported the present work.

References

[1] H. Sawa, S. Wakao, J. Furukawa, Denki Kagaku 58 (1990) 862.
[2] Y. Moriwaki, T. Gamo, H. Seri, T. Iwaki, J. Less-Common Met. 172–174 (1991) 1211.
[3] A. Zëttel, F. Meli, L. Schlapbach, J. Alloys Comp. 206 (1994) 31.
[4] M.A. Fetcenko, S. Venkatesan, S.R. Ovshinsky, Proc. Symp. on Hydrogen Storage Materials, Batteries and Electrochemistry 92–95 (1992) 141–167.
[5] C. Iwakura, T. Asaoka, H. Yoneyama, T. Sakai, H. Ishikawa, K. Oguro, Nippon Kagaku Kaishi (1988) pp. 1482–1488.
[6] J. Balej, Int. J. Hydrogen Energy 10 (1985) 365–374.
[7] C. Iwakura, I. Kim, N. Matsui, H. Inoue, M. Matsuoka, Electrochimica Acta 40 (1995) 561–566.
[8] C. Iwakura, T. Oura, H. Inoue, M. Matsuoka, Electrochimica Acta 41 (1996) 117–121.
[9] C. Iwakra, H. Kasuga, I. Kim, H. Inoue, M. Matsuoka, Electrochimica Acta 41 (1996) 2691–2694.
[10] D. Linden, Handbook of Batteries, 2nd edn., McGraw-Hill (1995) p. 14.22.
[11] C. Iwakura, Y. Kajiya, H. Yoneyama, T. Sakai, K. Oguro, H. Ishigawa, J. Electrochem. Soc. 136 (1989) 1351–1355.